Yavuz *et al. Journal of Ovarian Research* (2026) 19:152
https://doi.org/10.1186/s13048-026-02071-4

Journal of Ovarian Research

RESEARCH Open Access

Flunarizine attenuates ischemia–reperfusion–induced ovarian injury in rats

Arzu Yavuz[1], Kemine Uzel[1], Esra Tuba Sezgin[2], Şeyma İlayda Paltacı[3], Özlem Demir[4], Mehmet Kuzucu[5] and Halis Süleyman[6*]

Abstract

Background Ovarian ischemia–reperfusion (I/R) injury is associated with oxidative stress, inflammation, and histopathological damage. The aim of this study was to investigate the potential protective effects of flunarizine against ovarian I/R–induced injury in an experimental rat model.

Methods Rats were divided into four groups: healthy control (HG), sham-operated (SOG), ovarian ischemia–reperfusion (OIR), and flunarizine-treated OIR (FOIR). Ovarian tissues were analyzed in terms of oxidative stress markers, antioxidant enzyme activities, inflammatory cytokines, and histopathological alterations, including follicle counting.

Results Ovarian I/R significantly increased tissue levels of malondialdehyde (MDA), tumor necrosis factor-alpha (TNF-α), interleukin-1 beta (IL-1β), interleukin-6 (IL-6) while significantly decreasing total glutathione (tGSH), superoxide dismutase (SOD) and catalase (CAT) levels. Histopathological evaluation revealed severe follicular degeneration, interstitial edema, vascular congestion, and inflammatory cell infiltration in the OIR group. Following flunarizine administration, these biochemical and histopathological alterations were significantly ameliorated, and a partial restoration in follicle counts was observed.

Conclusion The findings of this study demonstrate that flunarizine exerts protective effects against ovarian I/R injury by reducing oxidative stress, inflammation, and histopathological damage.

Keywords Flunarizine, Ovarian ischemia–reperfusion, Rat, Oxidative stress, Inflammation, Follicle counting

Introduction

Ovarian ischemia is frequently encountered in clinical practice, most commonly as a consequence of ovarian torsion [1]. This pathological condition arises from the complete or partial rotation of the ovary around its vascular axis, resulting in a marked reduction or complete interruption of blood flow to the adnexa [2]. To address this condition, detorsion is recommended, as it restores perfusion to the affected ovary [3]. However, reperfusion following detorsion may paradoxically induce more severe tissue injury than ischemia alone, a phenomenon termed I/R injury [4]. In the existing literature, I/R injury is characterized as a complex

*Correspondence:
Halis Süleyman
halis.suleyman@gmail.com; esra.demir@erzincan.edu.tr
[1]Department of Obstetrics and Gynecology, SBU Kocaeli City Hospital, Kocaeli, Turkey
[2]Anesthesia Program, Vocational School of Health Services, Erzincan Binali Yıldırım University, Erzincan, Turkey
[3]Department of Obstetrics and Gynecology, Erzincan Binali Yıldırım University, Erzincan, Turkey
[4]Department of Histology and Embryology, Faculty of Medicine, Erzincan Binali Yıldırım University, Erzincan, Turkey
[5]Department of Biology, Faculty of Arts and Sciences, Erzincan Binali Yıldırım University, Erzincan, Turkey
[6]Department of Pharmacology, Faculty of Medicine, Erzincan Binali Yıldırım University, Erzincan, Turkey

© The Author(s) 2026. **Open Access** This article is licensed under a Creative Commons Attribution-NonCommercial-NoDerivatives 4.0 International License, which permits any non-commercial use, sharing, distribution and reproduction in any medium or format, as long as you give appropriate credit to the original author(s) and the source, provide a link to the Creative Commons licence, and indicate if you modified the licensed material. You do not have permission under this licence to share adapted material derived from this article or parts of it. The images or other third party material in this article are included in the article's Creative Commons licence, unless indicated otherwise in a credit line to the material. If material is not included in the article's Creative Commons licence and your intended use is not permitted by statutory regulation or exceeds the permitted use, you will need to obtain permission directly from the copyright holder. To view a copy of this licence, visit http://creativecommons.org/licenses/by-nc-nd/4.0/.

pathological cascade initiated by tissue hypoxia, followed by excessive production of reactive oxygen species (ROS) and further amplified by an inflammatory response [5]. Among the widely studied ROS are superoxide anion ($O_2\bullet^-$), hydroxyl radicals (•OH), hydrogen peroxide (H_2O_2), hypochlorous acid, and peroxynitrite derived from nitric oxide metabolism [6]. ROS produced at physiological levels play a critical role in cellular homeostasis and immune regulation, including inflammatory responses. In contrast, excessive ROS generation results in direct oxidative damage to biological macromolecules, such as proteins, nucleic acids, and lipids, thereby contributing to the development of inflammatory and degenerative tissue injury [7]. These ROS, commonly referred to as reperfusion mediators, initiate lipid peroxidation (LPO) of cell membrane lipids, leading to the formation of toxic by-products such as MDA [6]. Notably, MDA represents the principal end product of LPO and exhibits cytotoxic and genotoxic properties [8]. Consequently, elevated MDA levels—widely used as an indicator of oxidative stress—reflect increased ROS activity. Moreover, MDA itself may further aggravate cellular injury owing to its inherent toxicity [6].

The principal mechanisms underlying the pathogenesis of I/R injury involve depletion of intracellular energy reserves, inhibition of the Na^+/K^+-ATPase pump in the cell membrane, disruption of ionic homeostasis, and subsequent intracellular accumulation of Na^+ and Ca^{2+} ions [5]. Accordingly, current evidence suggests that therapeutic strategies aimed at attenuating tissue I/R injury may benefit from agents with antioxidant and anti-inflammatory properties, as well as those capable of blocking Na^+ and Ca^{2+} channels.

Flunarizine, which was investigated in the present study for its potential effects on ovarian I/R injury, is a lipophilic diphenylpiperazine derivative that functions as a Ca^{2+} and Na^+ channel inhibitor [9, 10]. It has been reported that flunarizine attenuates mitochondrial damage through its antioxidant properties and by enhancing ATP synthesis [11]. Furthermore, previous studies have demonstrated that flunarizine exerts anti-inflammatory and neuroprotective effects in addition to its antioxidant capacity [12]. Hirfanoglu et al. (2009) reported that the antimigraine efficacy of flunarizine may be attributed to its suppressive effects on pro-inflammatory cytokines, including TNF-α, IL-1β, and IL-6 [13].

Collectively, evidence from the literature suggests that flunarizine may have therapeutic potential in mitigating ovarian injury associated with I/R. However, data specifically addressing its effects on I/R-induced ovarian damage remain limited. Therefore, the present study aimed to evaluate the effects of flunarizine on ovarian injury induced by I/R in rats using both biochemical and histopathological analyses.

Materials and methods

Animals

The experimental study included a total of 24 female albino Wistar rats weighing between 266 and 278 g. These animals were obtained from the Erzincan Binali Yıldırım University Medical Experimental Application and Research Center. Prior to the initiation of the experimental procedures, all animals were housed in groups under standardized laboratory conditions, with a controlled ambient temperature of 22 °C and a 12-h light/dark cycle. All experimental protocols were reviewed and approved by the Local Animal Experimentation Ethics Committee (Approval Date: 25.12.2025, Meeting Number: 2025/12).

Chemicals

Flunarizine (5 mg tablets) was purchased from Johnson & Johnson Medical Products Industry and Trade Ltd. (İstanbul, Turkiye). Ketamine was supplied by Pfizer Pharmaceuticals Ltd. (Turkiye).

Animal groups

Female albino Wistar rats were randomly allocated into four experimental groups: HG, SOG, OIR, and FOIR.

Experimental procedure

The ovarian I/R procedure was performed under aseptic surgical conditions in a controlled laboratory environment. To ensure procedural reproducibility and minimize inter-operator variability, all surgical interventions were performed by a single surgeon.

Anesthesia was induced by intraperitoneal administration of ketamine (60 mg/kg) and maintained with intermittent sevoflurane inhalation. In accordance with previous studies, the immobile supine phase of anesthesia was considered appropriate for surgical intervention [14]. Body temperature was maintained throughout the procedure using a heating pad. Under anesthesia, the ovaries were accessed via a 2–2.5 cm vertical incision in the lower abdominal region. In the SOG group, the ovaries were explored and the incision was closed with surgical sutures without further manipulation to establish sham conditions. In the OIR and FOIR groups, the right ovary, together with the fallopian tube and vascular pedicle, was rotated 360° clockwise to induce torsion. The degree of torsion and the anatomical structures included were kept constant in all animals. Torsion was maintained for 3 h using atraumatic vascular clamps to produce a uniform ischemic insult. Following the ischemic period, the clamps were removed, detorsion was performed, and reperfusion was allowed for 6 h. Restoration of blood

flow was confirmed visually by color change and revascularization of the ovarian tissue. The reperfusion duration was selected to represent the acute phase of ovarian I/R injury based on previously published torsion–detorsion rat models [15]. The dose of flunarizine (5 mg/kg) was determined based on previous experimental studies demonstrating its efficacy and safety in I/R models. The drug was administered 1 h prior to anesthesia to ensure adequate systemic absorption [16]. An equivalent volume of distilled water was administered orally to the SOG ($n = 6$) and OIR ($n = 6$) groups via the same route. At the end of the reperfusion period, all animals were euthanized under high-dose ketamine anesthesia (120 mg/kg), and the ovaries were excised. Ovarian tissue samples were analyzed for MDA, tGSH, SOD, CAT, TNF-α, IL-6, and IL-1β levels. In addition, histopathological examinations of ovarian tissues were performed. The biochemical and histopathological findings obtained from all experimental groups were subsequently subjected to comparative analysis.

Biochemical analyses

Preparation of samples

Ovarian tissues were weighed and, at the end of the ischemia/reperfusion (I/R) protocol, were immediately snap-frozen in liquid nitrogen. All preparation steps were carried out on ice to maintain the cold chain. Frozen tissues were homogenized in a pre-cooled mortar under liquid nitrogen. The resulting tissue powder was suspended in phosphate-buffered saline (PBS; pH 7.4) containing a protease inhibitor cocktail at a tissue-to-buffer ratio of 1:10 (w/v). To ensure complete cellular disruption, homogenization was further performed at 4 °C using a homogenizer. The homogenates were vortexed for 10 s and then centrifuged at 10.000 rpm for 20 min at 4 °C. The supernatants obtained were carefully collected and aliquoted to prevent repeated freeze–thaw cycles. Samples were stored at – 80 °C until the time of analysis.

Tissue MDA, GSH, SOD, and CAT protein analysis

All biochemical parameters were analyzed using commercially available, rat-specific assay kits validated by the manufacturers and performed in accordance with the manufacturers' instructions. Tissue MDA, GSH, and SOD levels were quantified using ELISA kits supplied by Cayman Chemical Company (USA) (product numbers: 10009055, 703002, and 706002, respectively). Catalase (CAT) activity was determined spectrophotometrically according to the method described by Goth [17]. Tissue protein concentrations were measured using the Bradford method for normalization [18].

Tissue TNF-α, IL-1β, and IL-6 analysis

TNF-α, IL-1β, and IL-6 concentrations were measured using ELISA kits obtained from Eastbiopharm Co., Ltd. (China). Absorbance readings were performed at 450 nm using a microplate reader, and concentrations were calculated from standard calibration curves. All samples were analyzed in duplicate, and intra- and inter-assay coefficients of variation were < 10% as reported by the manufacturers.

Histopathological analysis

Ovarian tissue samples were fixed in 10% neutral-buffered formaldehyde for 72 h and subsequently washed with tap water for 24 h. The tissues were then processed through a graded series of ethanol solutions (70%, 80%, 90%, and 100%) for dehydration, cleared in xylene, and embedded in paraffin. Sections of 4 μm thickness were cut from paraffin blocks and stained with hematoxylin and eosin (H&E) according to the method described by Bancroft and Gamble (2008). The stained sections were examined and digitally photographed using a light microscope equipped with DP2-SAL software (Olympus Inc., Tokyo, Japan). For semiquantitative evaluation, one central region and five peripheral cortical regions were systematically selected from serial sections for each specimen to minimize sampling bias, and degenerative changes were scored within these areas. Ovarian tissue damage was assessed based on follicular degeneration, interstitial edema, vascular dilatation/congestion, and inflammatory cell infiltration. Each parameter was scored using a predefined four-point scale: 0, no damage; 1, mild damage; 2, moderate damage; and 3, severe damage. Representative histological reference features corresponding to each score were used to ensure consistency across evaluations. From serially sectioned samples taken from each rat, six non-overlapping fields were selected, and primordial follicles, developing follicles (primary, secondary, and tertiary follicles were classified as developing follicles), atretic follicles, and corpus luteum were counted at 100× magnification. To avoid double counting, follicles were recorded only when the oocyte nucleus was clearly visible within the section. Histopathological assessment and scoring were performed by an experienced histologist who was blinded to the experimental groups. All evaluations were conducted using standardized criteria applied uniformly to all specimens.

Statistical analyses

Statistical analyses were performed using SPSS software (version 22.0, IBM Corp., Armonk, NY, USA). Data were expressed as mean ± standard deviation (SD). The normality of data distribution was assessed using the Shapiro–Wilk test. Due to the small sample size and the lack of normal distribution, non-parametric statistical methods

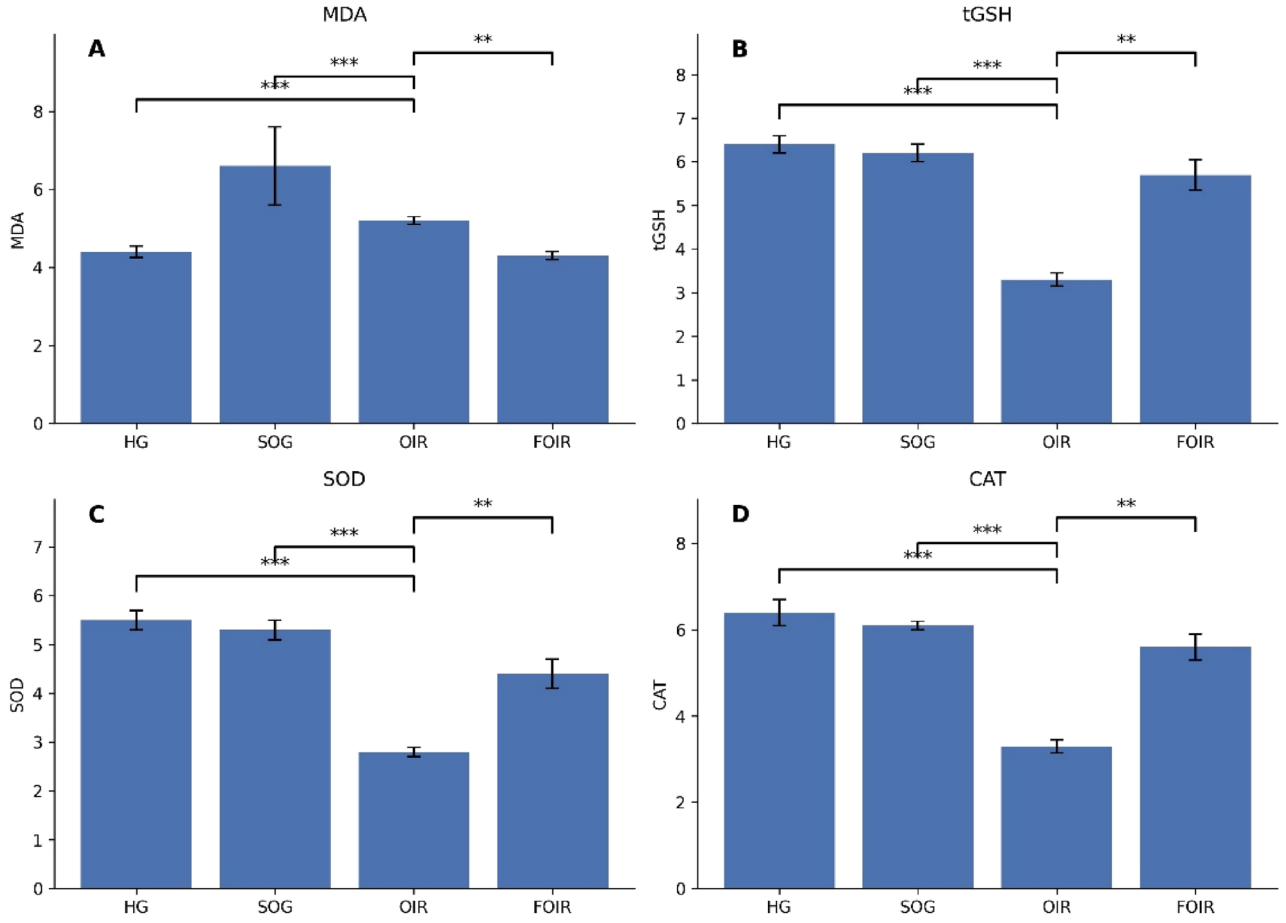


Fig. 1 Comparison of oxidative stress and antioxidant parameters among experimental groups. **A**. MDA, **B**. tGSH, **C**. SOD and **D**. CAT levels in experimental groups. Data are expressed as mean ± SD. Group differences were analyzed using the Kruskal–Wallis test. Post-hoc pairwise comparisons were performed using Dunn's test with Bonferroni correction. Statistical significance is indicated as follows: *p < 0.05, **p < 0.01, ***p < 0.001. Brackets denote statistically significant differences between groups

Table 1 Biochemical and Inflammatory Profiles of the Experimental Groups

Parameter	HG (Mean ± SD)	SOG (Mean ± SD)	OIR (Mean ± SD)	FOIR (Mean ± SD)	*p* value	Post-hoc lettering*
MDA	4.43 ± 0.16^{a}	6.64 ± 1.01^{d}	5.27 ± 0.10^{c}	4.28 ± 0.11^{b}	< 0.001	d > c > b ≈ a
tGSH	6.38 ± 0.19^{a}	6.16 ± 0.19^{a}	3.26 ± 0.13^{c}	5.74 ± 0.31^{b}	< 0.001	a > b > c
SOD	5.50 ± 0.21^{a}	5.31 ± 0.17^{a}	2.79 ± 0.12^{c}	4.35 ± 0.28^{b}	< 0.001	a > b > c
CAT	6.40 ± 0.29^{a}	6.13 ± 0.08^{a}	3.29 ± 0.17^{c}	5.61 ± 0.34^{b}	< 0.001	a > b > c
TNF-α	2.43 ± 0.15^{a}	2.55 ± 0.19^{a}	4.72 ± 0.19^{c}	2.92 ± 0.11^{b}	< 0.001	c > b > a
IL-1β	3.19 ± 0.13^{a}	3.47 ± 0.15^{a}	6.71 ± 0.11^{c}	3.94 ± 0.17^{b}	< 0.001	c > b > a
IL-6	1.84 ± 0.11^{a}	2.01 ± 0.26^{a}	4.40 ± 0.11^{c}	2.06 ± 0.19^{b}	0.0017	c > b > a

*Different superscript letters indicate statistically significant differences between groups according to Dunn's multiple comparison test with Bonferroni correction ($p < 0.05$). Data are expressed as mean ± SD

were applied. Differences among the groups were analyzed using the Kruskal–Wallis test. When a significant difference was detected, Dunn's multiple comparison test with Bonferroni correction was used for post-hoc analysis. A p value of less than 0.05 was considered statistically significant. Group differences identified in post-hoc comparisons were indicated using asterisk-based notation in figures and letter-based notation in tables.

Results

Biochemical findings

Analysis of MDA and tGSH levels in ovarian tissue

As illustrated in Fig. 1A; Table 1, ovarian tissue MDA levels did not differ significantly between the HG and SOG group ($p > 0.05$). Induction of I/R resulted in a significant increase in ovarian tissue MDA levels. This I/R-induced elevation in MDA was significantly attenuated by flunarizine treatment ($p < 0.001$).

Similarly, tGSH levels in ovarian tissue were comparable between the HG and SOG groups, with no statistically significant differences observed ($p > 0.05$). In contrast, the I/R procedure caused a marked reduction in tGSH levels, which was significantly reversed by flunarizine administration ($p < 0.001$) (Fig. 1B-Table 1).

Results of SOD and CAT analysis in ovarian tissue

Exposure of ovarian tissue to the I/R procedure led to a significant decrease in SOD levels. No significant difference in SOD levels was detected between the HG and SOG groups ($p > 0.05$). Flunarizine treatment significantly prevented the I/R-induced reduction in SOD levels ($p < 0.001$) (Fig. 1C-Table 1).

As illustrated in Fig. 1D; Table 1, CAT levels were significantly reduced following the I/R procedure. CAT levels did not differ significantly between the HG and SOG groups ($p > 0.05$). Administration of flunarizine significantly inhibited the I/R-associated decrease in CAT levels ($p < 0.001$).

TNF-α, IL-1β, and IL-6 levels in ovarian tissue

As shown in Fig. 2A, B and C, the I/R procedure resulted in significant elevations in ovarian tissue levels of the pro-inflammatory cytokines TNF-α, IL-1β, and IL-6. No statistically significant differences were observed between the healthy control and sham-operated groups for these cytokines. Flunarizine treatment significantly suppressed the I/R-induced increases in TNF-α, IL-1β, and IL-6 levels in ovarian tissue ($p < 0.001$) (Table 1).

Histopathological findings

As a result of histopathological evaluation, ovarian tissue samples from the HG group demonstrated a clear distinction between the cortical and medullary layers, with developing follicles (DF) and corpus luteum (CL) structures exhibiting a normal histological appearance. The interstitial connective tissue areas and blood vessels located in the medullary region displayed normal morphology (Fig. 3A). Similarly, ovarian tissue samples from the SOG group showed preserved cortical–medullary architecture comparable to that of the HG group, with developing follicular structures and cellular distribution exhibiting near-normal morphology. The interstitial connective tissue and blood vessels also appeared normal (Fig. 3B). In contrast, ovarian sections from the OIR group demonstrated a marked reduction in the number of DF compared with the HG and SOG groups, and some follicles contained clusters of cells

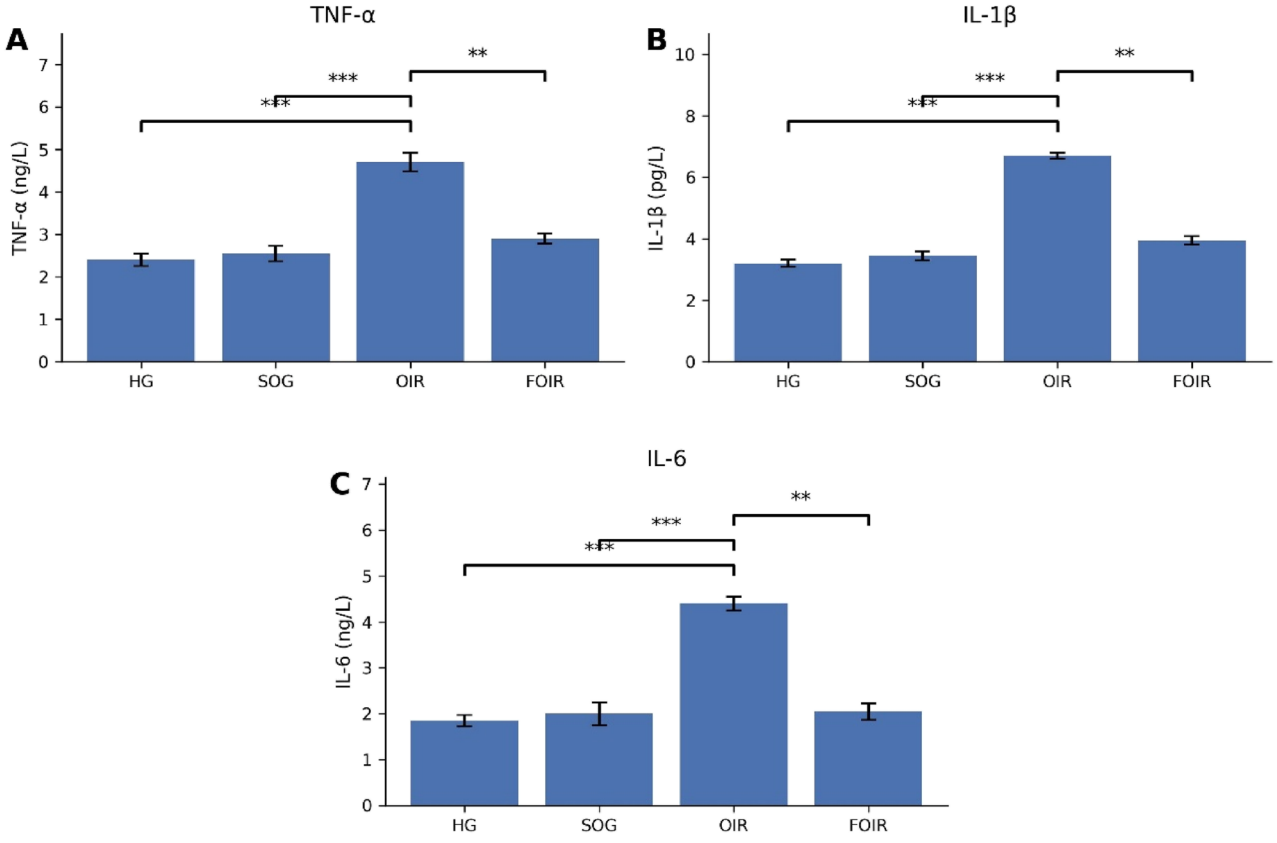


Fig. 2 Levels of pro-inflammatory cytokines in experimental groups. **A**. TNF-α (ng/L), **B**. IL-1β (pg/L), and **C**. IL-6 (ng/L) levels in experimental groups. Data are expressed as mean ± SD. Statistical analysis was performed using the Kruskal–Wallis test followed by Dunn's multiple comparison test with Bonferroni correction. Statistical significance is indicated as ***$p < 0.001$ and **$p < 0.01$. Brackets denote statistically significant differences between groups

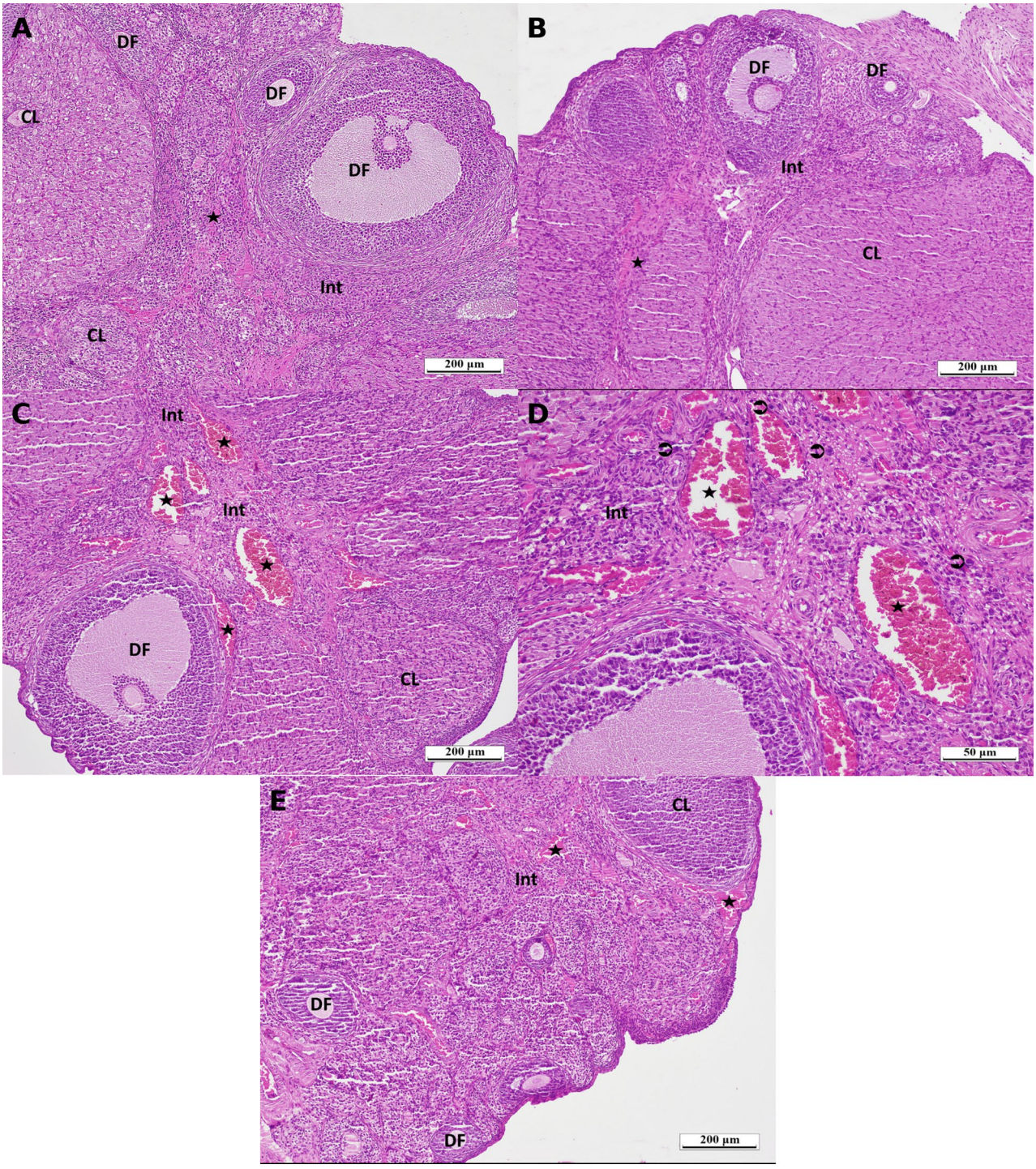


Fig. 3 Representative H&E-stained sections of ovarian tissue from the experimental groups. **A**. HG group: Ovarian tissue showing DF, interstitial area (Int), and CL; blood vessels are indicated by asterisks (*). Original magnification ×100. **B**. SOG group: Ovarian tissue exhibiting DF, Int, and CL; blood vessels are indicated by asterisks (*). Original magnification ×100. **C**. OIR group: Ovarian tissue demonstrating marked degeneration in DF, severe edema in the interstitial area (Int), and CL; severely dilated and congested blood vessels are indicated by asterisks (*). Original magnification ×100. **D**. OIR group (higher magnification): Pronounced interstitial edema (Int) with severely dilated and congested blood vessels (*), and inflammatory cell infiltration indicated by arrows (→). Original magnification ×200. **E**. FOIR group: Ovarian tissue showing DF, moderate interstitial edema (Int), and CL; moderately dilated and congested blood vessels are indicated by asterisks (*). Original magnification ×100

Table 2 Histopathological scores in ovarian tissues of experimental groups

Parametre	HG	SOG	OIR	FOIR	*p*
Follicular Degeneration	0 (0–1)[a]	0 (0–1)[a]	(2–3)[c]	1 (1–2)[b]	< 0.001
Interstitial edema	0 (0–0)[a]	0 (0–1)[a]	3 (2–3)[c]	1 (1–2)[b]	< 0.001
Vascular Dilatation / Congestion	0 (0–0)[a]	0 (0–1)[a]	3 (2–3)[c]	1 (1–2)[b]	< 0.001
Inflammatory cell infiltration	0 (0–0)[a]	0 (0–1)[a]	3 (2–3)[c]	1 (1–2)[b]	< 0.001

Values are expressed as median (min–max). Different superscript letters (a–c) indicate statistically significant differences between groups (Kruskal–Wallis test followed by Dunn's multiple comparison test, $p < 0.05$)

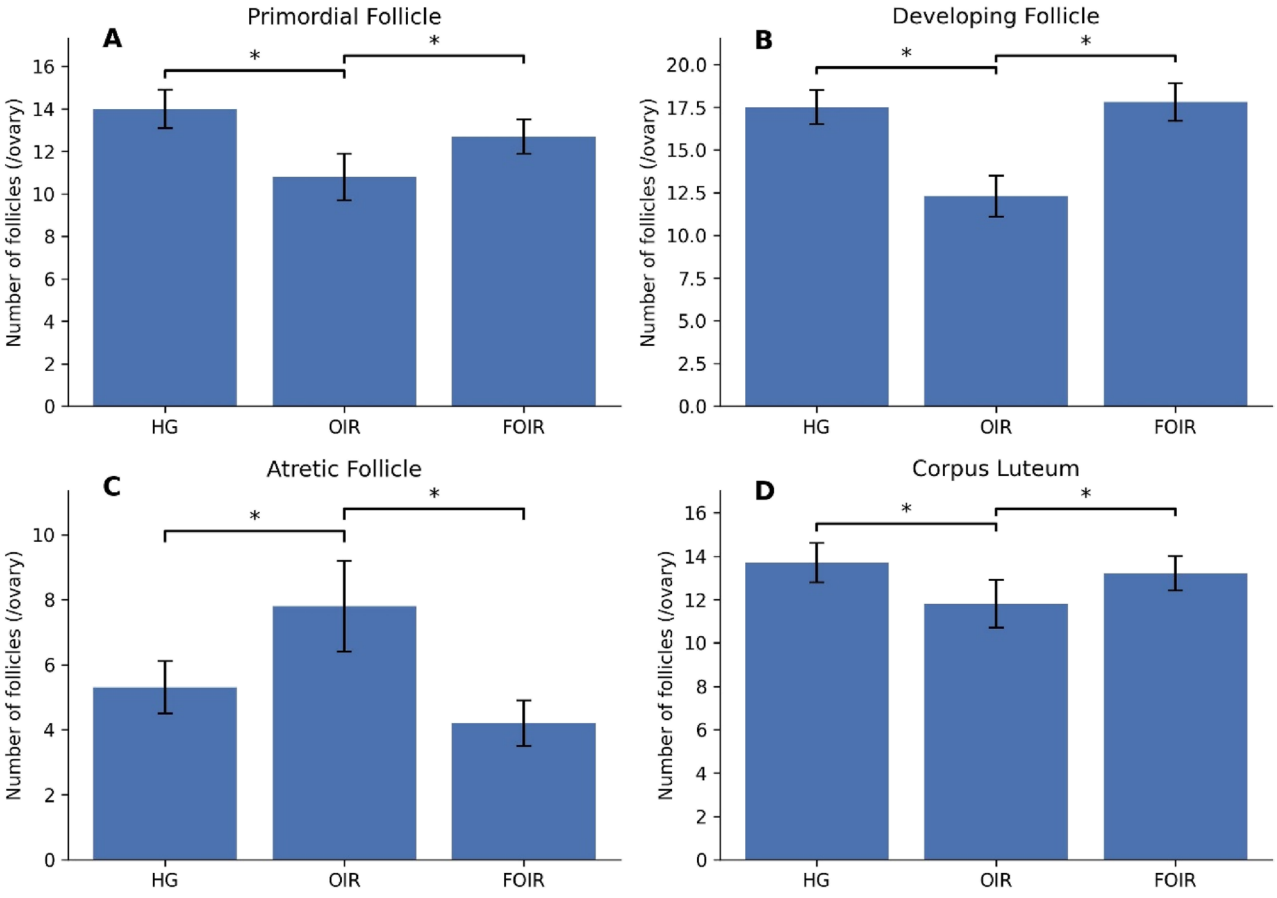


Fig. 4 Quantitative assessment of follicular structures in ovarian tissues. **A**. Primordial Follicle, **B**. Developing Follicle, **C**. Atretic Follicle, and **D**. Corpus Luteum in the HG, OIR, and FOIR groups. Data are presented as mean ± SD. Statistical analyses were performed using the Kruskal–Wallis test followed by Dunn's multiple comparison test with Bonferroni correction. Asterisks indicate statistically significant differences between the compared groups (*$p < 0.05$). Quantitative parameters in the SOG group did not differ significantly from the HG group and are therefore not shown

exhibiting necrotic features. Severe interstitial edema surrounding the follicles, together with pronounced vascular dilation and congestion, was observed (Fig. 3C). High-magnification examination further revealed dense inflammatory cell infiltration within the interstitial connective tissue and around blood vessels (Fig. 3D). In line with these findings, semi-quantitative histopathological scoring revealed a statistically significant decrease in developing follicle scores, accompanied by significant increases in interstitial edema, vascular dilation/congestion, and inflammatory cell infiltration scores in the OIR group compared with the HG and SOG groups ($p < 0.05$; Table 2). The quantitative findings were consistent with the histopathological observations. Follicle counting further supported these results, revealing statistically significant differences among the experimental groups (Fig. 4). In the OIR group, the number of primordial follicles was significantly reduced compared with the HG group ($p < 0.05$). In the FOIR group, primordial follicle counts were significantly increased compared with the OIR group ($p < 0.05$). The number of DF was significantly decreased in the OIR group compared with the HG group; in contrast, FOIR treatment significantly increased the number of DF compared with the OIR group ($p < 0.05$). The number of atretic follicles was significantly increased in the OIR group compared with the HG and FOIR groups; however, this increase observed in the OIR group was

significantly reduced following FOIR treatment ($p<0.05$). Similarly, the number of CL structures was significantly decreased in the OIR group compared with the HG group, whereas an improvement was observed in the FOIR group compared with the OIR group ($p<0.05$). In ovarian tissue samples from the FOIR group, the number of DF was relatively increased compared with the OIR group. Interstitial edema as well as vascular dilation and congestion persisted at mild to moderate levels compared with the OIR group (Fig. 3E). According to histopathological scoring, the FOIR group exhibited a significant increase in developing follicle scores and a significant reduction in other histopathological parameters compared with the OIR group ($p<0.05$).

Discussion

This study aimed to investigate the protective effects of flunarizine against I/R-induced ovarian injury in rats by integrating biochemical and histopathological assessments. The biochemical findings demonstrated that I/R exposure was associated with increased ovarian tissue levels of MDA, TNF-α, IL-1β, and IL-6, concomitant with significant reductions in tGSH, SOD, and CAT levels.

Collectively, these alterations indicate the presence of ovarian tissue injury characterized by enhanced oxidative stress and inflammation [19].

The reperfusion phase of I/R injury is well recognized to be associated with excessive production of ROS, which subsequently induces cellular injury through lipid peroxidation mechanisms [20, 21].

In this context, the observed elevation of MDA levels in ovarian tissue serves as a reliable biochemical indicator of LPO [22]. Accordingly, increased MDA concentrations reflect heightened ROS activity within the tissue. Moreover, lipid peroxidation–mediated injury is not limited to increased MDA production alone; MDA itself exerts cytotoxic effects that may further aggravate cellular damage [6]. These findings are consistent with previously reported data on ovarian I/R injury, supporting the validity of the experimental model used in the present study [23, 24].

Both enzymatic and non-enzymatic antioxidant defense systems play a critical role in protecting tissues against oxidative injury. GSH, a key non-enzymatic antioxidant, contributes to cellular redox homeostasis by scavenging reactive oxygen species [25]. Melekoğlu et al. (2018) reported a significant reduction in tGSH levels in an ovarian I/R model. In line with these observations, the present study demonstrated a marked decrease in tGSH levels following ovarian I/R, consistent with prior findings in the literature [26].

In parallel with the depletion of tGSH, significant reductions in the activities of the antioxidant enzymes SOD and CAT were observed in ovarian tissue subjected to I/R. These enzymes constitute essential components of the enzymatic antioxidant defense system, and impairment of their activity predisposes tissues to oxidative stress and subsequent injury [27]. Previous studies by Bozkurt et al. (2012) and Melekoğlu et al. (2018) similarly reported pronounced decreases in SOD and CAT levels following ovarian I/R, corroborating the results obtained in the current investigation [28]. Furthermore, the absence of significant differences between the healthy control and sham-operated groups with respect to oxidant and antioxidant parameters suggests that anesthesia and surgical manipulation alone did not induce measurable oxidative injury.

In ovarian tissue exposed to I/R, there is a notable increase in the levels of TNF-α, IL-1β, and IL-6, which coincides with heightened oxidant activity and diminished antioxidant defenses. These pro-inflammatory cytokines are known to contribute to fever, inflammation, and tissue damage [29]. In the present study, the rise in TNF-α, IL-1β, and IL-6 levels in the ovarian I/R injury model aligns with findings from earlier research [30]. This observation is further supported by Naykı et al. (2018), who reported elevated TNF-α and IL-1β levels under similar conditions, as well as Dincer et al. (2022), who noted increased expression of TNF-α, IL-1β, and IL-6 in ovarian tissue following I/R injury [15, 31]. The elevated levels of these cytokines suggest that the tissue damage is not merely a consequence of oxidative stress but is closely tied to a significant inflammatory response. In contrast, cytokine levels did not differ significantly between the sham-operated and healthy control groups, further supporting the specificity of the I/R-induced inflammatory changes observed in this model.

Tissue I/R injury is underpinned by several additional pathophysiological mechanisms, including depletion of cellular energy stores, inhibition of the Na^+/K^+-ATPase pump, and subsequent intracellular accumulation of Na^+ and Ca^{2+} ions [5]. Accordingly, evidence from the literature indicates that therapeutic approaches combining antioxidant and anti-inflammatory properties with Na^+ and Ca^{2+} channel blockade may confer protective effects against tissue I/R injury. Flunarizine, which has been proposed as a potential protective agent against ovarian I/R injury, is a lipophilic diphenylpiperazine derivative with inhibitory effects on Ca^{2+} and Na^+ channels [9, 10]. Its pharmacological profile demonstrates the capacity to attenuate mitochondrial damage through antioxidant and anti-inflammatory actions, while simultaneously enhancing ATP production [11, 12]. Ciancarelli et al. (2004) reported that the elevation in thiobarbituric acid reactive substances (TBARS) levels, which are indicative of MDA, was reduced following flunarizine administration [32]. In addition, flunarizine has been shown to ameliorate I/R-associated decreases in GSH levels and SOD activity, thereby limiting oxidative stress [33].

Zhu et al. (2022) further demonstrated that flunarizine attenuated inflammatory responses by preventing elevations in TNF-α and IL-6 concentrations [34]. Moreover, suppression of the pro-inflammatory cytokine IL-1β by flunarizine has been reported across various experimental models [35], and its role in preserving CAT activity through support of antioxidant defense mechanisms has also been documented [36]. In line with these reports, the present study demonstrated that flunarizine administration effectively mitigated oxidative stress and inflammatory responses associated with ovarian I/R injury.

The biochemical alterations observed in ovarian tissues subjected to I/R were closely paralleled by the histopathological findings. In animals exposed exclusively to I/R, a pronounced reduction in follicle number, follicular cell necrosis, marked interstitial edema, and substantial vascular dilatation and congestion were evident. In addition, dense polymorphonuclear leukocyte infiltration indicated activation of a robust inflammatory response. These histopathological alterations were further supported by quantitative follicle counting, which demonstrated a significant reduction in primordial and primary follicle numbers in the I/R group, along with altered secondary and antral follicle distributions. Flunarizine treatment partially restored follicle counts across different developmental stages, indicating preservation of follicular dynamics following I/R injury. Consistent with these observations, previous studies have reported that ovarian I/R induces histopathological disturbances characterized by edema, hemorrhage, follicular degeneration, and inflammation [37–39]. Flunarizine treatment attenuated these I/R-associated histopathological alterations. Given that mitochondrial dysfunction and Ca^{2+} overload are recognized as key contributors to ovarian tissue damage following I/R, the observed histological improvements may be attributable to the Ca^{2+} channel–blocking properties of flunarizine and its capacity to modulate mitochondrial integrity. Supporting this interpretation, Bhattacharya et al. (2025) demonstrated that flunarizine ameliorated mitochondrial dysfunction in an experimental model of ischemic stroke, suggesting mechanistic pathways that may similarly underlie the reduction of I/R-associated histopathological damage in ovarian tissue [40]. No histopathologically significant differences were observed between the healthy control and sham-operated groups, further indicating that the surgical procedure alone did not induce overt tissue injury.

Conclusion

This study demonstrated the protective effects of flunarizine against I/R-induced ovarian injury in rats using biochemical and histopathological approaches. The findings showed that I/R exposure induced pronounced oxidative stress and an inflammatory response in ovarian tissue, whereas flunarizine administration significantly attenuated these I/R-associated alterations. These biochemical improvements were accompanied by marked amelioration of histopathological damage.

The observed protective effects of flunarizine are likely mediated, at least in part, through its inhibitory actions on Ca^{2+} and Na^{+} channels, consistent with its known pharmacological properties. In addition, flunarizine exerts multi-target protective actions through mitochondrial stabilization, regulation of intracellular calcium homeostasis, and antioxidant mechanisms. Unlike conventional antioxidant agents, it preserves mitochondrial membrane integrity by modulating disrupted calcium balance during ischemia and contributes to the maintenance of cellular energy metabolism. This effect profile enables modulation of the early pathophysiological processes of I/R injury. Taken together, the present findings provide experimental evidence that flunarizine confers protection against ovarian I/R injury at both the biochemical and histopathological levels. Accordingly, flunarizine exhibited protective effects against ovarian tissue damage associated with I/R in the present experimental model, and further studies are needed to clarify its potential clinical applicability.

Limitations

This study has several limitations that should be acknowledged. First, only a single dose and administration protocol of flunarizine was evaluated, which precludes assessment of dose–response relationships. In addition, the relatively small sample size per group ($n = 6$) may limit the statistical power of the findings. Although key biochemical and histopathological markers related to oxidative stress and inflammation were examined, detailed molecular and mechanistic pathways were not directly investigated. Specifically, apoptosis-related markers such as caspase activation, Bcl-2/Bax balance, and cytochrome c release, as well as mitochondrial functional parameters and calcium signaling pathways, which may play critical roles in I/R injury, were not evaluated. Furthermore, hormonal parameters and fertility-related outcomes were not assessed, limiting conclusions regarding the long-term effects of flunarizine on ovarian function, ovarian reserve, and reproductive potential. Accordingly, further studies incorporating long-term follow-up and functional reproductive endpoints are warranted. Additionally, effect size measures and confidence intervals were not calculated due to the exploratory design and limited sample size, which may represent a statistical reporting limitation. Finally, as the present investigation was conducted in an experimental animal model, clinical studies are required to determine the translational relevance of these findings to human ovarian I/R injury.

Abbreviations

I/R	Ischemia–reperfusion
ROS	Reactive oxygen species
LPO	Lipid peroxidation
MDA	Malondialdehyde
tGSH	Total glutathione
SOD	Superoxide dismutase
CAT	Catalase
TNF- α	Tumor necrosis factor-alpha
IL-1B	Interleukin-1 beta
IL-6	Interleukin-6

Acknowledgements
Not applicable.

Authors' contributions
A.Y. contributed to the conceptualization, literature search and analysis, original draft writing, and visualization. K.U. was involved in conceptualization, manuscript review and editing, and visualization. E.T.S. participated in original draft writing, statistical and biochemical analyses, manuscript review, editing. Ş.İ.P. contributed to the manuscript review and editing. Ö.D. participated in histopathological analyses, provided supervision. M.K biochemical analyses, contributed to manuscript review and editing. original draft. H.S. contributed to the conceptualization, literature search and analysis. All authors have read and approved the final version of the manuscript.

Funding
This research received no external funding.

Data availability
The datasets used and/or analyzed during the current study are available from the corresponding author upon reasonable request.

Declarations

Ethics approval and consent to participate
All animal experimental procedures were approved by the Erzincan Binali Yıldırım University Animal Experiments Local Ethics Committee (Approval Date: 25.12.2025, Meeting Number: 2025/12) and conducted in accordance with institutional and international guidelines.

Consent for publication
Not applicable.

Competing interests
The authors declare no competing interests.

Received: 14 January 2026 / Accepted: 10 March 2026
Published online: 17 March 2026

References

1. Beaunoyer M, Chapdelaine J, Bouchard S, et al. Asynchronous bilateral ovarian torsion. J Pediatr Surg. 2004;39:746–8.
2. Spinelli C, Piscioneri J, Strambi S. Adnexal torsion in adolescents: update and review of the literature. Curr Opin Obstet Gynecol. 2015;27(5):320–5. https://doi.org/10.1097/GCO.0000000000000197.
3. Celik A, Ergun O, Aldemir H, et al. Long-term results of conservative management of adnexal torsion in children. J Pediatr Surg. 2005;40:704–8.
4. Kumbasar S, Cetin N, Yapca OE, et al. Exogenous ATP administration prevents ischemia/reperfusion-induced oxidative stress and tissue injury by modulation of hypoxanthine metabolic pathway in rat ovary. Cienc Rural. 2014;44(7):1257–63. https://doi.org/10.1590/0103-8478cr20131006.
5. Yapca OE, Borekci B, Suleyman H. Ischemia–reperfusion damage. Eurasian J Med. 2013;45(2):126–7. https://doi.org/10.5152/eajm.2013.24.
6. Suleyman H, Ozcicek A. Molecular mechanism of ischemia–reperfusion injury. Arch Basic Clin Res. 2020;2(1):25–7.
7. Liu J, Han X, Zhang T, et al. Reactive oxygen species scavenging biomaterials for anti-inflammatory diseases: from mechanism to therapy. J Hematol Oncol. 2023;16:116. https://doi.org/10.1186/s13045-023-01512-7.
8. Li Pomi F, Gammeri L, Borgia F, et al. Oxidative stress and skin diseases: the role of lipid peroxidation. Antioxidants (Basel). 2025;14(5):555. https://doi.org/10.3390/antiox14050555.
9. Leone M, Grazzi L, La Mantia L, Bussone G. Flunarizine in migraine: a minireview. Headache. 1991;31(6):388–91. https://doi.org/10.1111/j.1526-4610.1991.hed3106388.x.
10. Shinde V, Yegnanarayan R, Shah P, et al. Antidepressant-like activity of flunarizine in rats. N Am J Med Sci. 2015;7(3):100–3. https://doi.org/10.4103/1947-2714.153921.
11. Muthuraman A, Sood S, Singla SK, et al. Ameliorative effect of flunarizine in cisplatin-induced acute renal failure via mitochondrial permeability transition pore inactivation in rats. Naunyn Schmiedebergs Arch Pharmacol. 2011;383(1):57–64. https://doi.org/10.1007/s00210-010-0572-z.
12. Muthuraman A, Singla SK, Peters A. Exploring the potential of flunarizine for cisplatin-induced painful uremic neuropathy in rats. Int Neurourol J. 2011;15(3):127–34. https://doi.org/10.5213/inj.2011.15.3.127.
13. Hirfanoglu T, Serdaroglu A, Gulbahar O, Cansu A. Prophylactic drugs and cytokine and leptin levels in children with migraine. Pediatr Neurol. 2009;41(4):281–7. https://doi.org/10.1016/j.pediatrneurol.2009.04.019.
14. Demiryilmaz I, Turan MI, Kisaoglu A, et al. Protective effect of nimesulide against hepatic ischemia–reperfusion injury in rats. Pharmacol Rep. 2014;66(4):647–52. https://doi.org/10.1016/j.pharep.2014.02.015.
15. Nayki C, Nayki U, Keskin Cimen F, et al. Effect of rutin on ovarian ischemia–reperfusion injury. Gynecol Endocrinol. 2018;34(9):809–14.
16. Gulati P, Muthuraman A, Kaur P. Investigation of the role of non-selective calcium channel blocker (flunarizine) on cerebral ischemic–reperfusion associated cognitive dysfunction in aged mice. Pharmacol Biochem Behav. 2015;131:26–32. https://doi.org/10.1016/j.pbb.2015.01.015.
17. Goth L. A simple method for determination of serum catalase activity. Clin Chim Acta. 1991;196:143–51.
18. Bradford MM. A rapid and sensitive method for the quantitation of microgram quantities of protein. Anal Biochem. 1976;72:248–54.
19. Karakus S, Dogan HO, Ozkaraca M. Protective effect of cloprostenol on ovarian ischemia/reperfusion injury in rats. Transpl Immunol. 2024;86:102108.
20. Karateke F, Karateke A, Topdagi B, et al. The role of mannitol and vitamin D in ovarian ischemia/reperfusion injury in rats with acute abdominal. Curr Issues Mol Biol. 2024;46(8):8903–13.
21. Mohammadi Z, Hosseinianvari S, Ghazalian N, et al. Impact of chrysin on folliculogenesis and ovarian apoptosis in ischemia–reperfusion injury. Int J Fertil Steril. 2022;16(4):299–305.
22. Ayala A, Munoz MF, Arguelles S. Lipid peroxidation mechanisms of malondialdehyde. Oxid Med Cell Longev. 2014;2014:360438. https://doi.org/10.1155/2014/360438.
23. Toktay E, Tastan TB, Gurbuz MA, et al. Protective effect of astaxanthin on ovary ischemia–reperfusion injury. Iran J Basic Med Sci. 2022;25(2):173–8.
24. Aksak Karamese S, Toktay E, Unal D, et al. Protective effects of beta-carotene against ovarian ischemia–reperfusion injury. Acta Histochem. 2015;117(8):790–7.
25. Ono H, Sakamoto A, Sakura N. Plasma total glutathione concentrations in epileptic patients. Clin Chim Acta. 2000;298(1–2):135–43.
26. Melekoglu R, Ciftci O, Eraslan S, et al. The protective effects of glycyrrhetinic acid and chrysin against ischemia-reperfusion injury in rat ovaries. Biomed Res Int. 2018;2018:5421308. https://doi.org/10.1155/2018/5421308.
27. Yenkoyan K, Harutyunyan H, Harutyunyan A. Role of SOD/CAT imbalance in autism spectrum disorders. Free Radic Biol Med. 2018;123:85–95.
28. Bozkurt S, Arikan DC, Kurutas EB, et al. Selenium protects against ovarian ischemia–reperfusion injury. J Pediatr Surg. 2012;47(9):1735–41.
29. Dinarello CA. Proinflammatory cytokines. Chest. 2000;118(2):503–8.
30. Uzel K, Lakhno I, Turkler C, et al. Tocilizumab prevents ovarian ischemia–reperfusion injury. An Acad Bras Cienc. 2023;95(1):e20220442.
31. Dincer B, Cinar I, Yayla M, et al. Protective effects of gossypin on ovarian ischemia/reperfusion injury. J Obstet Gynaecol Res. 2022;48(3):748–56.
32. Ciancarelli I, Tozzi-Ciancarelli MG, Di Massimo C, et al. Flunarizine effects on oxidative stress in migraine patients. Cephalalgia. 2004;24(7):528–32.
33. Muthuraman A, Ramesh M, Chauhan A. Mitochondrial dependent apoptosis: ameliorative effect of flunarizine on ischemia-reperfusion of celiac artery-induced gastric lesions in rats. Dig Dis Sci. 2011;56(8):2244–51.
34. Zhu J, Chen J, Zhang K. Flunarizine combined with duloxetine in chronic migraine. Brain Behav. 2022;12(8):e2689.
35. So H, Kim H, Kim Y, et al. Cisplatin-induced auditory damage: role of proinflammatory cytokines. J Assoc Res Otolaryngol. 2008;9(3):290–306.

36. Singha HA, Sengupta M, Bawari M. Biochemical alterations and ameliorative effect of flunarizine. J Appl Biol Biotechnol. 2021;9(3):66–74.
37. Demir M, Yilmaz B, Kalyoncu S, et al. Metformin reduces ovarian ischemia/reperfusion injury. Taiwan J Obstet Gynecol. 2021;60(1):45–50.
38. Arslan S, Aşır F, Özkorkmaz EG, Azizoğlu M, Başuguy E, Okur MH, et al. Protective effects of Passiflora incarnata on ovarian ischemia/reperfusion damage in rats with ovarian torsion. Ulus Travma Acil Cerrahi Derg. 2023;29(12):1344. https://doi.org/10.14744/tjtes.2023.52986.
39. Toktay E, Gurbuz M, Bal T, et al. Protective effect of daidzein on ovarian ischemia/reperfusion injury in rats. Cukurova Med J. 2022;47(1):1–7.
40. Bhattacharya P, Saraf S, Barik A, et al. Mitochondrial dysfunction alleviated after ischemic stroke. Neurosci Lett. 2025;138410.

Publisher's note

Springer Nature remains neutral with regard to jurisdictional claims in published maps and institutional affiliations.